0026-895X/08/7404-1008–1021$20.00
MOLECULAR PHARMACOLOGY
Copyright © 2008 The American Society for Pharmacology and Experimental Therapeutics
Mol Pharmacol 74:1008–1021, 2008

Vol. 74, No. 4
49676/3386915
Printed in U.S.A.

Structural Motifs of Importance for the Constitutive Activity of the Orphan 7TM Receptor EBI2: Analysis of Receptor Activation in the Absence of an Agonist[S]

Tau Benned-Jensen and Mette M. Rosenkilde

Laboratory for Molecular Pharmacology, Department of Neuroscience and Pharmacology, Faculty of Health Sciences, the Panum Institute, Copenhagen University, Copenhagen, Denmark.

Received June 13, 2008; accepted July 15, 2008

ABSTRACT

The Epstein-Barr induced receptor 2 (EBI2) is a lymphocyte-expressed orphan seven transmembrane-spanning (7TM) receptor that signals constitutively through $G\alpha_i$, as shown, for instance by guanosine 5′-*O*-(3-thio)triphosphate incorporation. Two regions of importance for the constitutive activity were identified by a systematic mutational analysis of 29 residues in EBI2. The cAMP response element-binding protein transcription factor was used as a measure of receptor activity and was correlated to the receptor surface expression. PheVI:13 (Phe^{257}), and the neighboring CysVI:12 (Cys^{256}), in the conserved CW/FxP motif in TM 6, acted as negative regulators as Ala substitutions at these positions increased the constitutive activity 5.7- and 2.3-fold, respectively, compared with EBI2 wild type (wt). In contrast, ArgII:20 (Arg^{87}) in TM-2 acted as a positive regulator, as substitution to Ala, but not to Lys, decreased the constitutive activity more than 7-fold compared with wt EBI2. IleIII:03 (Ile^{106}) is located only 4 Å from ArgII:20, and a favorable electrostatic interaction with ArgII:20 was created by introduction of Glu in III:03, given that the activity increased to 4.4-fold of that wt EBI2. It is noteworthy that swapping these charges by introduction of Glu in II:20 and Arg in III:03 resulted in a 2.7-fold increase compared with wt EBI2, thereby rescuing the two signaling-deficient single mutations, which exhibited a 3.8- to 4.5-fold decrease in constitutive activity. The uncovering of these molecular mechanisms for EBI2 activation is important from a drug development point of view, in that it may facilitate the rational design and development of small-molecule inverse agonists against EBI2 of putative importance as antiviral- or immune modulatory therapy.

G protein-coupled seven transmembrane α-helix-spanning receptors (7TM receptors) constitute one of the largest superfamilies of proteins in the human genome and are targets for >30% of all drugs on the market. The endogenous ligands are highly diverse and span from photons, metals, nucleotides, biogenic amines, amino acids, peptides, and proteins to lipids, steroids, and Krebs-cycle intermediates. Approximately 750 7TM receptors have been identified in the human genome, including ~350 olfactory and ~30 other chemosensory receptors. The nonolfactory and nonchemosensory receptors are divided into four families: classes A (rhodopsin-like), B, C, and F/S (Frizzled), of which class A is by far the largest (284 members). The EBI2 receptor was identified in 1993 as one of the most up-regulated genes in lymphocytes infected with Epstein-Barr virus (EBV; hence the name Epstein-Barr induced receptor 2, EBI2) (Birkenbach et al., 1993). It is expressed predominantly in lymphoid tissue and constitutes one of ~150 orphan receptors within class A (Vassilatis et al., 2003). Despite this, it was recently described to signal with high constitutive activity through $G\alpha_i$ (Rosenkilde et al., 2006).

Constitutive activity is a well known phenomenon among 7TM receptors, and occurs within wild-type (wt) as well as mutated receptors, although it should be noted that in vitro observed constitutive activity could also result from artificial receptor overexpression (Seifert and Wenzel-Seifert, 2002). However, the fact that constitutive activity has been associated with multiple diseases [for instance, retinitis pigmentosa (rhodopsin mutations), pigmentation defects (melanocyte-stimulating hormone receptor muta-

This work was supported from the Danish Medical Research Council, the NovoNordisk Foundation, the Carlsberg Foundation, and the Aase and Ejnar Danielsen Foundation, the AP-Moller foundation and the European Community's Sixth Framework Program (INNOCHEM: LSHB-CT-2005-518167).

Article, publication date, and citation information can be found at http://molpharm.aspetjournals.org.

doi:10.1124/mol.108.049676.

[S] The online version of this article (available at http://molpharm.aspetjournals.org) contains supplemental material.

ABBREVIATIONS: 7TM, seven transmembrane; EBV, Epstein-Barr virus; EBI2, Epstein-Barr induced receptor 2; wt, wild-type; GTPγS, guanosine 5′-*O*-(3-thio)triphosphate; HEK, human embryonic kidney; CREB, cAMP response element-binding protein; GFP, green fluorescent protein; PBS, phosphate-buffered saline; BSA, bovine serum albumin; Gqi4myr, Gαq6qi4myr; ECL2, extracellular loop-2.

tions), and hyperfunctional thyroid adenomas (thyroid-stimulating hormone receptor mutations) (Robbins et al., 1993; Parma et al., 1995)] supports a biological relevance, at least in these receptors. It is noteworthy that constitutive activity is a hallmark for the majority of herpesvirus-encoded 7TM receptors, exemplified by the broad-spectrum activity of ORF74 from human herpesvirus 8 and the selective constitutive activity through $G\alpha_i$ of the EBV-encoded BILF-1 receptor (Bais et al., 1998; Rosenkilde et al., 1999; Beisser et al., 2005; Paulsen et al., 2005). The >200-fold induction of EBI2 expression upon EBV cell entry is the only known modulation of EBI2 (Birkenbach et al., 1993), and the biologic function therefore remains to be described. Because of the orphan status, the only pharmacologic "handle" at present is the constitutive activity.

The molecular mechanism behind 7TM receptor activation has been a major area of research for many years and was advanced by the crystal structure of bovine rhodopsin in 2000 (Palczewski et al., 2000) and the crystal structures of the β2-adrenergic receptor published in 2007 (Cherezov et al., 2007; Rasmussen et al., 2007). Based on these crystals and on mutational analysis with, for example, metal-ion site engineering and disulfide engineering or biophysical experiments in for example rhodopsin and the adrenergic receptors, a toggle switch model has been proposed in which the transmembrane helices move during receptor activation in a way that creates space for the G protein and/or adaptor protein at the intracellular edge, whereas extracellular segments of the helices approach each other (Shi et al., 2002; Hubbell et al., 2003; Elling et al., 2006; Schwartz et al., 2006).

In the present study, we focus on the molecular mechanism behind the constitutive activity of EBI2 (Fig. 1) and show, in addition, that this activity can be measured as an increase in GTPγS-binding in EBI2-expressing lymphocytes and HEK293 cells (Fig. 2). In contrast to most other rhodopsin-like receptors, EBI2 is not part of any larger subfamily (Vassilatis et al., 2003), and the closest human homolog is GPR18, with which it shares only 23.1% homology and 40.2% similarity. Although EBI2 lacks obvious homology-partners, it still contains the conserved residues identified in most

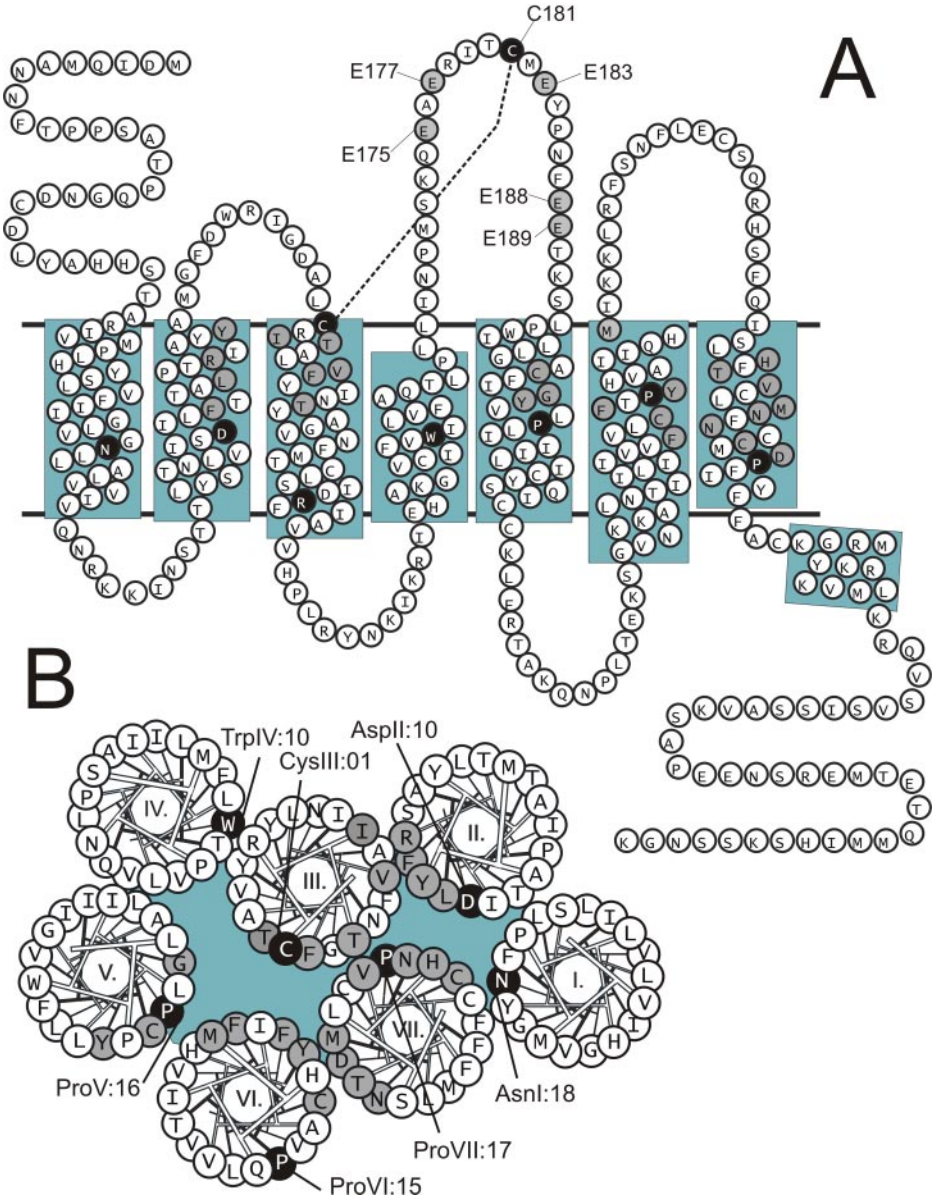

Fig. 1. Serpentine (A) and helical wheel (B) models of the human EBI2 receptor. Gray circles indicate mutated residues substituted to either reduce or increase the size of the side chain or to change the charge. Black background with white letter indicates the most conserved residues in each helix. In addition, the positions of the conserved amino acids are indicated next to the black circles.

other rhodopsin-like 7TM receptors (Asn I:18, Asp II:10, Cys III:01, Trp IV:10, and the three prolines in positions V:16, VI:15, and VII:17) (Fig. 1). [In the text, we use the generic 7TM numbering system suggested by Baldwin (1993) and later modified by Schwartz (1994), whereas in the tables, we also include the nomenclature suggested by Ballesteros and Weinstein (1995).] We created 44 mutations in 29 residues located in the transmembrane helices based on the proposed models for receptor activation within class A (Hubbell et al., 2003; Schwartz et al., 2006) (Fig. 1). The residues were chosen based on their prevalence in class A or their being part of well known functional motifs. Side-chain elimination with Ala substitution was used most frequently. However, in certain cases, we introduced residues with similar chemical properties (for instance, Phe to Trp or Arg to Lys), changed charge (for instance, Arg to Glu), or introduced size in a steric hindrance approach (for instance, introduction of Trp). Consistent with the current models for receptor activation, we find that the CWxP motif in TM-6 (in EBI2 CFxP) regulates receptor activation; in addition, we identify Arg^{87} (in position II:20) as being important for maintenance of the high constitutive activity of EBI2.

Materials and Methods

Materials. EBI2 was kindly provided by H.R. Luttichau, Laboratory for Molecular Pharmacology, and corresponded to the GenBank accession number L08177. The promiscuous chimeric G protein GαΔ6qi4myr (abbreviated Gqi4myr) was kindly provided by Evi Kostenis (Rheinische Friedrich-Wilhelm University, Bonn, Germany). Lipofectamine 2000 reagent and Opti-MEM were purchased from Invitrogen (Carlsbad, CA). LucLite (lyophilized substrate solution) was from PerkinElmer Life and Analytical Sciences (Waltham, MA). Goat anti-mouse horseradish peroxidase-conjugated antibody was from Pierce (Rockford, IL), whereas mouse anti-FLAG (M1) antibody, forskolin, and pertussis toxin were from Sigma Chemicals Co. (St. Louis, MO). Both SlowFade Antifade reagent and goat anti-mouse Alexa Fluor 488-conjugated antibody were from Invitrogen. 3,3′,5,5′-Tetramethylbenzidine substrate was purchased from KemEnTech (Taastrup, Denmark).

Site-Directed Mutagenesis. All EBI2 constructs were inserted into a modified pcDNA3 vector, kindly provided by Kate Hansen (7TM Pharma, Horsholm, Denmark), which contained an upstream sequence encoding a hemagglutinin signal peptide fused to the FLAG tag. Site-directed mutagenesis was carried out using the *Pfu* polymerase (Stratagene, La Jolla, CA), and the generated mutations were verified by bidirectional DNA sequencing at MWG Biotech (Martinsried, Germany).

Transfection and Tissue Culture. HEK293 cells were grown in Dulbecco's modified Eagle's medium adjusted to contain 4500 mg/liter glucose (Invitrogen), 10% fetal bovine serum, 180 u/ml penicillin, and 45 μg/ml streptomycin at 10% CO_2 and 37°C. Stably transfected HEK293 cells were grown in the same medium, but with G418 added at 800 mg/ml, as were stably transfected TREX-HEK293 cells but with blasticidin and Zeocin (both from Invitrogen) added at 5 and 100 μg/ml, respectively. L1.2 pre-B cells were grown in RPMI 1640 medium supplemented with 10% FBS, 180 u/ml penicillin, 45 μg/ml streptomycin, and 800 mg/ml G418 at. For transient transfections, the Lipofectamine 2000 reagent in the serum-free medium Opti-MEM was used according to the manufacturer's description. In brief, the cells were transfected for 5 h at 37°C using Lipofectamine 2000 at 12 μl/ml and DNA at varying concentrations and subsequently incubated in fresh growth medium for 48 h before usage. Cells were always transfected in parallel for the CREB luciferase assay and enzyme-linked immunosorbent assay (ELISA). HEK293 and TREX-HEK293 clones stably expressing FLAG-tagged wt EBI2 were generated by transfecting the cells with FLAG-tagged wt EBI2 cloned into pcDNA3.1 or pcDNA4/TO, respectively, and selected using G418

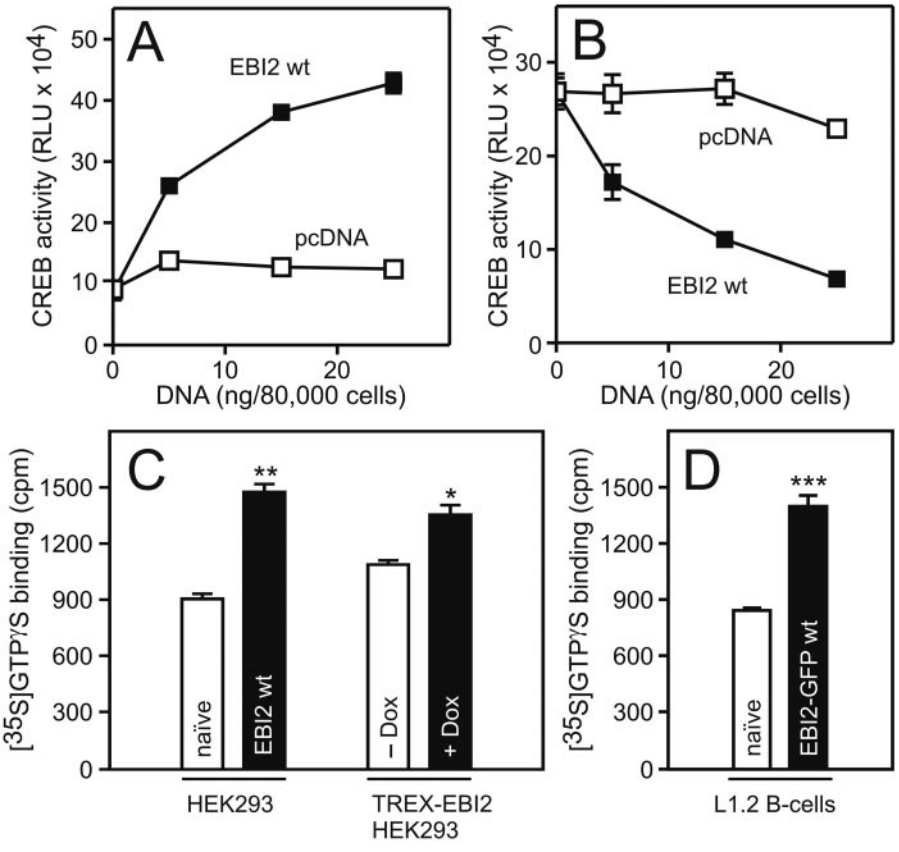

Fig. 2. EBI2 is a constitutively active 7TM receptor. A, HEK293 cells were transiently transfected with Gqi4myr, reporter plasmid (CREB/Luc system), and increasing concentrations of FLAG-tagged EBI2 receptor or pcDNA (0, 5, 15, and 25 ng/8 × 10^4 cells). A representative example is shown. B, HEK293 cells were transiently transfected with reporter plasmid (CREB/Luc system) and increasing concentrations of FLAG-tagged EBI2 receptor or pcDNA (0, 5, 15, and 25 ng/8 × 10^4 cells). On the assay day, the cAMP production was induced by incubating the cells in growth medium containing 15 μM forskolin. A representative example is shown. C, [^{35}S]GTPγS binding to membranes isolated from naive HEK293 cells and HEK293 cells stably expressing FLAG-tagged EBI2 receptor (left) or induced (+Dox; doxycycline at 5 ng/ml) or uninduced (−Dox) TREX-HEK293 cells stably transfected with FLAG-tagged EBI2 receptor (right). The data are mean ± S.E.M of three independent experiments performed in triplicate. *, $p < 0.05$; **, $p < 0.01$. D, [^{35}S]GTPγS binding to membranes isolated from naive L1.2 pre-B-cells and L1.2 cells stably expressing C-terminally GFP-tagged EBI2 receptor. The data are mean ± S.E.M of three independent experiments performed in triplicates. ***, $p < 0.001$.

or Zeocin. The L1.2 pre-B cell line stably expressing a wt EBI2-GFP fusion protein was generated as described previously (Rosenkilde et al., 2006).

Membrane Preparation. Membranes were prepared from naive HEK293 cells, HEK293 cells stably expressing FLAG-tagged wt EBI2, naive L1.2 pre-B-cells, L1.2. cells stably expressing C-terminally GFP-tagged wt EBI2, and induced or uninduced TREX-HEK293 stably transfected with FLAG-tagged wt EBI2. In the latter case, the expression of the receptor was induced by incubating the cells in growth medium containing 5 ng/ml doxycycline (Invitrogen) for 48 h. The cells were manually harvested with a rubber policeman in ice-cold PBS and homogenized on ice with the use of a Dounce homogenizer. The homogenate was centrifuged at 500 rpm for 3 min at 4°C. Subsequently, the supernatants were collected and centrifuged at 20,000 rpm at 4°C. The resulting membrane pellets were resuspended in 20 mM HEPES buffer containing 2 mM $MgCl_2$ and Complete protease inhibitor mixture (Roche, Mannheim, Germany) and kept at −80°C until subjected to [^{35}S]GTPγS binding experiments. The protein concentrations in each preparation were determined using the BCA protein assay kit (Pierce, Rockford, IL).

[^{35}S]GTPγS Binding Assay. [^{35}S]GTPγS binding experiments were carried out in white 96-well plates (NUNC A/S, Roskilde, Denmark) using the scintillation proximity assay-based method. A volume of membrane preparation (corresponding to 20 μg protein/well) was diluted in assay buffer (final concentrations: 50 mM HEPES, 2 mM $MgCl_2$, 50 mM NaCl, 1 mM EGTA, 1 μM GDP, 0.1% BSA, and Complete inhibitor mix). [^{35}S]GTPγS (1250 Ci/mmol; 12.5 mCi/ml; PerkinElmer Life and Analytical Sciences) diluted in assay buffer was added to a final concentration of 1 nM and incubated 30 min at room temperature. Subsequently, wheat germ agglutinin-coupled scintillation proximity assay beads (GE Healthcare, Chalfont St. Giles, Buckinghamshire, UK) were added (final concentration, 2.8 mg/ml) followed by 30-min incubation at room temperature on a plate shaker. Finally, the plates were centrifuged at 1500 rpm for 5 min, and the amount of radioactivity determined using a TopCount scintillation counter (PerkinElmer Life and Analytical Sciences). The level of unspecific binding was determined by adding unlabeled GTPγS at a final concentration of 40 μM.

CREB Trans-Reporting Luciferase Assay. The signaling was determined using the trans-reporting CREB-luciferase assay according to the manufacturer's recommendations (Stratagene, La Jolla, CA). Cells were seeded at 8×10^4 cells/well in 96-well culture plates 24 h before transfection and were transfected with the trans-activator plasmid pFA2-CREB and the reporter plasmid pFRLUC at 6 ng/8×10^4 cells (i.e., 6 ng/well) and 50 ng/8×10^4 cells (i.e., 50 ng/well), respectively. In most experiments (Figs. 3–7), the cells were cotransfected with the chimeric G-protein GαΔ6qi4myr (abbreviated Gqi4myr) at 30 ng/8×10^4 cells, (Kostenis, 2002). However, as a more direct measurement of cAMP inhibition, forskolin (15 μM) was added instead of Gqi4myr, and the effect of increasing concentrations of receptor DNA on cAMP-induced CREB-activation was measured (Fig. 9) in the absence or presence of pertussis toxin (100 ng/ml). The CREB activity was determined 48 h after transfection using the LucLite substrate (PerkinElmer Life and Analytical Sciences). In brief, the cells were washed twice in Dulbecco's PBS (0.9 mM $CaCl_2$, 2.7 mM KCl, 1.5 mM KH_2PO_4, 0.5 mM $MgCl_2$, 137 mM NaCl, and 8.1 mM Na_2HPO_4), and the luminescence was measured in a microplate scintillation and luminescence counter (TopCount) after 10-min incubation in 100 μl of Dulbecco's PBS and 100 μl of LucLite substrate. Every receptor construct was tested in parallel with EBI2 wt receptor at least thrice in quadruples.

Enzyme-Linked Immunosorbent Assay. HEK293 cells were transiently transfected with the indicated FLAG-tagged EBI2 constructs using Lipofectamine 2000 as described above. Forty-eight hours after transfection, the cells were fixed in 4% glutaraldehyde for 10 min, washed thrice in TBS, and blocked for 30 min with TBS containing 2% BSA. Subsequently, the cells were incubated with mouse anti-FLAG M1 antibody at 2 μg/ml for 2 h in TBS supplemented with 1% BSA and 1 mM $CaCl_2$. After three washes in TBS containing 1% BSA and 1 mM $CaCl_2$, the cells were incubated for 1 h with goat anti-mouse horseradish peroxidase-conjugated antibody diluted 1:1000 in the same buffer as the primary antibody. After washing, the immune reactivity was determined by addition of 3,3′,5,5′-tetramethylbenzidine according to manufacturer's instructions. All steps were carried out at room temperature.

Data Handling. The relative constitutive activity, given as mean ± S.E.M. in -fold compared with wt, is calculated by normalizing the CREB signaling (CS) to cell surface expression (SE) as measured by ELISA according to the following equations: (1) Constitutive activity (CA) = CS/SE and (2) $CA_{mut,relative} = CA_{mut}/CA_{wt} = (CS_{mut} \times SE_{wt})/(SE_{mut} \times CS_{wt})$.

Statistical Analysis. All statistical analyses were performed as the Student's *t* tests.

Immunocytochemistry. HEK293 cells were seeded on poly-L-lysine-coated coverslips in six-well plates at 5×10^5 cells/well. The following day, the cells were transfected with the indicated FLAG-tagged EBI2 constructs at 150 ng/well using Lipofectamine 2000 as described above. Forty-eight hours after transfection, the specimens were fixed in 4% paraformaldehyde for 15 min, washed thrice in TBS, and blocked for 20 min with TBS (0.05 M Tris Base and 0.9% NaCl, pH 7.6) containing 2% BSA. Receptors residing at the cell surface were labeled by incubation with mouse anti-FLAG M1 antibody at 2 μg/ml in TBS containing 1% BSA and 1 mM $CaCl_2$ for 1 h. After three washes with TBS containing 1 mM $CaCl_2$, labeled receptors were detected by incubating with goat anti-mouse Alexa Fluor 488-conjugated IgG antibody diluted 1:1000 in TBS containing 1% BSA and 1 mM $CaCl_2$ for 30 min. After washing, the specimens were mounted in SlowFade Antifade reagent using nail polish as sealing. Mock transfected cells were included to ensure no unspecific binding of either primary or secondary antibodies. All steps were performed at room temperature.

Confocal Microscopy. Confocal microscopy was performed using a LSM 510 laser-scanning unit coupled to an inverted microscope with a 63 × 1.4 NA oil immersion Plan-Apochromat objective (Carl Zeiss GmbH, Jena, Germany). Alexa Fluor 488 was excited using an argon-krypton laser (λ = 488 nm), and the emission was collected with a long-pass filter at 505 nm. Images were recorded in 1024 × 1024 pixels and averaged over 16 whole-frame scans.

Results

Constitutive Activity of wt EBI2 through GTPγS Binding. One of the most widely used methods to determine receptor activation of G proteins is the measurement of [^{35}S]GTPγS binding. The previously shown constitutive activity of EBI2 through $G\alpha_i$ (Rosenkilde et al., 2006) (as summarized in Fig. 2, A and B) was supported by a significant increase in [^{35}S]GTPγS binding in membranes from HEK293 cells stably expressing EBI2 or expressing EBI2 under the tetracycline-inducible promoter (TREX-system) compared with naive HEK293 cells or uninduced EBI2 TREX-HEK293 cells. (Fig. 2C). This was also shown in membranes from L1.2 lymphocytes stably expressing EBI2 fused with GFP (Fig. 2D). In all cases, the receptor was well expressed at the surface as demonstrated by ELISA (HEK293) or confocal microscopy (L1.2) (data not shown).

Structural Motifs of Importance for the Constitutive Activity. No endogenous or exogenous ligands have yet been identified for EBI2. We therefore normalized the signaling activity to surface expression to compare mutations with each other. Consequently, all mutations were created with an N-terminal M1 FLAG tag, which did not affect EBI2 signaling (Rosenkilde et al., 2006), and the cell-surface expression was quantified in HEK293 cells transiently transfected with

0, 15, and 25 ng of receptor DNA by an ELISA technique using the M1 anti-FLAG antibody as primary and the horseradish peroxidase-conjugated antibody as secondary antibody. The constitutive activity through $G\alpha_i$ was measured in HEK293 cells as the activation of the transcription factor CREB in the presence of Gqi4myr (a chimeric $G\alpha$ subunit that is recognized by $G\alpha_i$-coupled receptors but activates $G\alpha_q$-regulated downstream pathways) (Kostenis, 2002) at four receptor concentrations (0, 5, 15, and 25 ng/8 $\times$ 10^4 cells). For all mutations, the relative constitutive activity was determined by correlating the activity to the surface expression at 15 and 25 ng of receptor DNA/8 $\times$ 10^4 cells (Tables 1 and 2).

TM-6 Is Involved in the Regulation of Constitutive Activity. The motif including the conserved Pro in TM-6 (CFxP in EBI2) was changed into the most frequently occurring CWxP-motif by mutating PheVI:13 (Phe^{257}) to Trp, F(VI:13)W-EBI2. It is noteworthy that this substitution had no effect on the constitutive activity of EBI2 (Fig. 3A, Table 1). In contrast, introduction of Ala substantially increased the activity by 5- to 6-fold, and introducing a polar residue (Cys) resulted in a similar increase (3- to 4-fold) (Fig. 3A, Table 1). Contrary to the Trp introduction, which only slightly decreased the surface expression (to 73% of wt EBI2), a huge decrease was observed for the Ala and Cys introductions (7 and 17% of wt EBI2; Fig. 3C, Table 1). Despite this, these receptors could still be observed on the surface by confocal microscopy using an antibody against the N-terminal Flag-tag and a secondary Alexa Fluor 488-conjugated antibody (Fig. 3, D–F).

Linearity is a prerequisite for the correlation of receptor activity with surface expression. Therefore, before the mutational screening, we performed 12-point gene-dose experiments ranging from 1 to 35 ng of wt EBI2 receptor per 8 $\times$ 10^4 cells and determined receptor activity as well as surface expression for all doses. As seen in Fig. 4A, there was an almost linear correlation (r^2 = 0.94) between receptor activity and surface expression within the chosen DNA concentrations (see supplemental Fig. 1, A and B, for the corresponding CREB-activity and expression measurements, respectively). However, at very low (1 ng/8 $\times$ 10^4 cells) and very high (30–35 ng/8 $\times$ 10^4 cells) DNA concentrations, a tendency of lower activity per expressed molecule was observed. This could be due to a higher threshold for the measurement of activation compared with surface expression for the low DNA concentration, and a saturation of the CREB-activation pathway for the high DNA concentrations. However, at between 5 and 25 ng of receptor DNA, we observed a linearity that validated the correlation of receptor activity with surface expression within these concentrations. Because the increases in relative activity for the Ala and Cys introductions in VI:13 were mainly determined by a very low receptor expression (Fig. 3, A–C), we included multiple gene doses (see Supplemental Fig. 2) for F(VI:13)A-EBI2 and F(VI:13)C-EBI2 and adjusted to exactly the same expression level as wt EBI2. For identical expression levels (Fig. 4B, white bars), an increase in activity appeared (Fig. 4B, black bars) that was similar to that obtained from the correlation of expression and activity for fixed DNA concentrations (Table 1, Fig. 3A).

Effect of Aromatic Residues in TM-5 and -6 in the Vicinity of PheVI:13 on EBI2 Signaling. The aromatic

TABLE 1

Mutations in the EBI2 major binding pocket

EBI2 mutations were assessed for their cell surface expression and ability to activate the CREB transcription factor in transiently transfected HEK293 cells. The table shows these values at 15 ng/8 $\times$ 10^4 cells and the relative constitutive activity (see *Materials and Methods* for calculation) at 15 and 25 ng/8 $\times$ 10^4 cells. CREB activity and cell surface expression are presented as percentage ± S.E.M., whereas the relative constitutive activity is presented as -fold ± S.E.M. In all cases, the results are given relative to the wt value. The number of experiments is given as *n*. Receptor residues are presented according to the Schwartz and Ballesteros/Weinstein (Ballest.) nomenclatures (see Introduction). Furthermore, the three most common amino acids at the particular position are given.

	Residue					CREB Activity	Expression	Relative CA		*n*
	Mutation	Number	Schwartz	Ballest	Three Most Common AAs	15 ng/well		15 ng	25 ng	
						%		*-fold*		
TM III	T(III:04)A	Thr107	Thr III:04	T3.28	V, 19%; S, 10%; W, 10%	97 ± 3.2	94 ± 1.6	1.0 ± 0.05	1.1 ± 0.07	3
	T(III:04)E					76 ± 12	53 ± 11	1.4 ± 0.08	1.2 ± 0.06	4
	F(III:08)A	Phe111	Phe III:08	F3.32	D, 20%; F, 15%; L, 9%	78 ± 10	108 ± 18	0.74 ± 0.05	0.82 ± 0.04	6
	F(III:08)Y					73 ± 11	39 ± 6.4	1.9 ± 0.11	1.8 ± 0.14	6
	T(III:12)A	Thr115	Thr III:12	T3.36	M, 20%; L, 15%; V, 11%	116 ± 10	126 ± 31	0.93 ± 0.07	1.2 ± 0.09	3
	T(III:12)F					142 ± 41	31 ± 91	0.46 ± 0.01	0.68 ± 0.09	4
TM V	C(V:09)A	Cys201	Cys V:09	C5.43	F, 23%; L, 13%; S, 10%	45 ± 5.9	71 ± 7.5	0.63 ± 0.07	0.68 ± 0.07	4
	G(V:12)W	Gly204	Gly V:12	C5.46	G, 29%; L, 14%; A, 11%	40 ± 2.7	66 ± 5.2	0.61 ± 0.03	0.64 ± 0.04	4
	Y(V:13)A	Tyr205	Tyr V:13	C5.47	F, 70%; Y, 11%; L, 4%	38 ± 4.7	54 ± 9.2	0.70 ± 0.08	0.64 ± 0.03	4
	Y(V:13)F					86 ± 7.3	61 ± 14	1.4 ± 0.13	1.4 ± 0.10	4
TM VI	F(VI:09)A	Phe253	Phe VI:09	F6.44	F, 82%; Y, 6%; L, 3%	75 ± 1.4	81 ± 8.9	0.91 ± 0.10	1.0 ± 0.07	5
	C(VI:12)A	Cys256	Cys VI:12	C6.47	C, 74%; S, 9%; F, 5%	95 ± 1.8	41 ± 1.6	2.3 ± 0.21[a]	2.4 ± 0.19[a]	4
	F(VI:13)A	Phe257	Phe VI:13	F6.48	W, 71%; F, 16%; Q, 2%	39 ± 7.5	7.0 ± 1.1	5.7 ± 0.50[b]	4.7 ± 0.27[b]	5
	F(VI:13)C					54 ± 8.3	17 ± 1.8	3.1 ± 0.27[a]	4.8 ± 0.27[b]	6
	F(VI:13)W					67 ± 5.3	73 ± 11	0.9 ± 0.08	1.0 ± 0.13	4
	Y(VI:16)A	Tyr260	Tyr VI:16	Y6.51	Y, 36%; F, 30%; L, 12%	25 ± 3.6	57 ± 7.3	0.43 ± 0.04	0.53 ± 0.07	6
	Y(VI:16)F					49 ± 4.7	96 ± 15	0.53 ± 0.03	0.59 ± 0.14	5
	M(VI:24)A	Met268	Met VI:24	M6.59	A, 16%; T, 14%; L, 12%	89 ± 4.7	109 ± 9.2	0.82 ± 0.07	0.84 ± 0.07	5
TM VII	T(VII:05)A	Thr293	Thr VII:05	T7.38	T, 24%; A, 15%; S, 13%	99 ± 7.1	126 ± 8.0	0.87 ± 0.05	0.69 ± 0.13	6
	V(VII:06)A	Val294	Val VII:06	V7.39	L, 21%; V, 11%; T, 11%	110 ± 11	88 ± 5.9	1.3 ± 0.07	1.4 ± 0.10	4
	M(VII:09)A	Met297	Met VII:09	M7.42	A, 40%; G, 20%; S, 13%	65 ± 2.3	93 ± 2.2	0.71 ± 0.02	0.78 ± 0.05	4
	M(VII:09)F					85 ± 15	80 ± 2.9	1.1 ± 0.06	1.4 ± 0.15	4
	N(VII:12)A	Asn300	Asn VII:12	N7.45	N, 67%; S, 12%; H, 9%	103 ± 5.8	146 ± 20	0.73 ± 0.08	0.81 ± 0.11	3

[a] Mutations with values (at both gene doses) between 2.00 and 4.00.
[b] Mutations with values (at both gene doses) above 4.00.

environment surrounding VI:13 in the major binding pocket is important for agonist-dependent, as well as constitutive activity in many receptors (see *Discussion*). [Due to the orphan status of EBI2, the term "major binding pocket" is used in a broader perspective, as robust experimental evidence support that the helices in rhodopsin-like 7TM receptors form a major and a minor binding pocket (delimited by TM-3 to -7 in the case of the major and TM-1 to -3 and TM-7 for the minor binding pocket).] In TM-5, position V:13 is highly conserved as an aromatic residue being either Phe (70%) or Tyr (11%) as in EBI2 and has been suggested to be part of an aromatic cluster of importance for receptor activity (Schwartz et al., 2006). In EBI2, however, only a 1.4-fold reduction in constitutive activity compared with wt activity was obtained upon substitution of Tyr^{205} to Ala, whereas introduction of Phe resulted in a modest increase in the relative activity of 1.4-fold (Table 1). In TM-6, two other highly conserved aromatic residue important for activity in some receptors (see *Discussion*) are found in the vicinity of PheVI:13: TyrVI:16 and PheVI:09 located one helical turn above and below, respectively (Fig. 1B). However, no effect was observed for F(VI:09)A-EBI2 (Fig. 5, A–C, Table 1). In contrast, an Ala-substitution of TyrVI:16 resulted in a decrease in relative constitutive activity of 2.3-fold. A similar decrease (1.9-fold) was obtained by introducing Phe at this position (Fig. 5, A–C, Table 1), indicating that the hydroxyl group influences receptor activity.

CysVI:12 has been suggested to act in concert with the aromatic residue in position VI:13 in the β2-adrenergic receptor (that holds a Trp in VI:13) (Shi et al., 2002). We therefore substituted it to Ala and interestingly observed a large increase in the constitutive activity (2.3-fold relative to wt EBI2) (Table 1). MetVI:24 is another residue of note in TM-6 as this position very seldom (only in 2%) holds a Met. We therefore introduced an Ala (the most common amino acid at this position) and observed no change in the activity or expression [i.e., no change in the relative constitutive activity (Table 1)].

Effect of Residues in TM-3, -5, and -7 Facing into the Major Binding Pocket on Receptor Activation. Biophysical evidence indicates that TM-7 and TM-3 move in concert with TM-6 during receptor activation (Farrens et al., 1996). We therefore substituted a total of six residues in the extracellular segments of these two helices pointing toward the major binding pocket (PheIII:08 and ThrIII:12 in TM-3 and ThrVII:05, ValVII:06, MetVII:09, and AsnVII:12 in TM-7). Collectively, these six Ala mutations had no major effect (a factor of <1.5) on the relative constitutive activity (Table 1). In more detail, the residue in III:08 is often aromatic (23%) and as such is part of the aromatic cluster (see *Discussion*). However, in EBI2, an Ala in III:08 decreased the activity only slightly (1.3-fold), whereas introduction of Tyr resulted in an 1.9-fold increase compared with wt EBI2 (Table 1). Met infrequently occurs at position VII:09 (1%), which usually contains Ala (40%) or Gly (20%). Nevertheless, substitution to Ala resulted in only a minor decrease in constitutive activity (1.4-fold), whereas introduction of Phe resulted in a minor increase in relative constitutive activity (to 1.1-fold; Fig. 5, D–F). Likewise, introduction of Ala in position VII:06 resulted in a minor increase in the relative constitutive activity

TABLE 2

Mutations in the EBI2 minor binding pocket and extracellular loop 2

EBI2 mutations were assessed for their cell surface expression and ability to activate the CREB transcription factor in transiently transfected HEK293 cells. The table shows these values at 15 ng/8 $\times$ 10^4 cells and the relative constitutive activity (see *Materials and Methods* for calculation) at 15 and 25 ng/8 $\times$ 10^4 cells. CREB activity and cell surface expression are presented as percentage $\pm$ S.E.M., whereas the relative constitutive activity is presented as fold $\pm$ S.E.M. In all cases, the results are given relative to the wt value. The number of experiments is given as *n*. Receptor residues are presented according to the Schwartz and Ballesteros/Weinstein (Ballest.) nomenclatures (see Introduction). Furthermore, the three most common amino acids at the particular position are given.

	Residue				CREB Activity	Expression	Relative CA		*n*
	Mutation	Number	Schwartz	Ballest	Three Most Common AAs	15 ng/well		15 ng	25 ng	
						%		*-fold*		
TM II	F(II:13)A	Phe80	Phe II:13	F2.53	V, 24%; F, 19%; L, 17%	97 ± 8.8	108 ± 7.7	0.90 ± 0.05	0.86 ± 0.02	6
	L(II:17)A	Leu84	Leu II:17	L2.57	L, 39%; V, 14%; C, 12%	93 ± 7.3	103 ± 8.8	0.90 ± 0.04	0.81 ± 0.03	4
	R(II:20)A	Arg87	Arg II:20	R2.60	L, 20%; F, 16%; W, 15%	9.1 ± 1.4	70 ± 13	0.14 ± 0.02[a]	0.16 ± 0.03[a]	5
	R(II:20)E					21 ± 3.6	77 ± 3.0	0.26 ± 0.04[b]	0.40 ± 0.04[b]	4
	R(II:20)K					76 ± 7.9	88 ± 13	0.86 ± 0.06	0.86 ± 0.07	4
	Y(II:24)A	Tyr91	Tyr II:24	Y2.64	Y, 21%; V, 13%; L, 10%	108 ± 19	107 ± 19	1.0 ± 0.07	1.0 ± 0.15	7
TM III	I(III:03)A	Ile106	Ile III:03	I3.27	L, 31%; V, 21%; P, 14%	89 ± 7.5	77 ± 11	1.2 ± 0.06	1.1 ± 0.13	3
	I(III:03)E					26 ± 3.8	6.0 ± 1.0	4.4 ± 0.09[d]	3.8 ± 0.19[c]	3
	I(III:03)R					4.2 ± 0.6	19 ± 1.6	0.22 ± 0.04[a]	0.20 ± 0.05[a]	6
	V(III:07)A	Val110	Val III:07	V3.31	L, 39%; I, 15%; V, 12%	108 ± 10	94 ± 6.5	1.2 ± 0.07	1.2 ± 0.07	5
TM VII	H(VII:03)A	His291	His VII:03	H7.36	L, 12%; I, 7%; H, 7%	52 ± 5.7	51 ± 11	0.97 ± 0.16	0.87 ± 0.07	3
	N(VII:10)A	Asn298	Asn VII:10	N7.43	Y, 33%; F, 14%; S, 13%	95 ± 5.9	111 ± 12	0.86 ± 0.08	0.94 ± 0.08	4
	N(VII:10)Y					37 ± 9.8	81 ± 4.1	0.44 ± 0.07[b]	0.44 ± 0.08[b]	4
	C(VII:14)A	Cys302	Cys VII:14	C7.47	C, 42%; A, 11%; V, 10%	51 ± 4.8	60 ± 10	0.86 ± 0.07	1.1 ± 0.07	4
Double	R(II:20)E-I(III:03)R	Arg087-Ile106	Arg II:20-Ile III:03	R2.60-I3.27		19 ± 0.6	7.1 ± 0.8	2.7 ± 0.29[d]	2.2 ± 0.18[d]	3
	R(II:20)E-I(III:03)E					3.6 ± 1.6	6.2 ± 0.9	0.55 ± 0.17	0.69 ± 0.11	3
ECL2	E183A					45 ± 3.7	61 ± 7.0	0.76 ± 0.02	0.69 ± 0.05	7
	E175A-E177A					89 ± 3.4	80 ± 8.9	1.1 ± 0.09	1.3 ± 0.04	3
	E188A-E189A					95 ± 4.2	69 ± 9.3	1.3 ± 0.16	1.3 ± 0.03	4
	E175A-E177A-E183A					47 ± 6.0	64 ± 7.9	0.74 ± 0.01	0.58 ± 0.07	3
	E183A-E188A-E189A					42 ± 2.6	77 ± 2.6	0.54 ± 0.02	0.51 ± 0.03	3

[a] Mutations with values (at both gene doses) between 0 and 0.25.
[b] Mutations with values (at both gene doses) between 0.25 and 0.50.
[c] Mutations with values (at both gene doses) between 2.00 and 4.00.
[d] Mutations with values (at both gene doses) above 4.00.

(1.3-fold of wt EBI2) (Fig. 5D). The expression levels of these mutations in VII:06 and VII:09 were similar to that of wt EBI2 (Fig. 5F).

In contrast to TM-3, -6, and -7, the role of TM-5 in receptor activation is poorly defined, although position V:13 may have an important role in some receptors (Schwartz et al., 2006). Position V:12, which protrudes right into the major binding pocket, is conserved as a small amino acid (Gly in 29% and Leu in 14%), and in some receptors, introduction of larger side chains abolishes receptor activity (Jensen et al., 2008). Despite this, we observed only a minor decrease (1.6-fold) for the substitution of Gly for Trp in V:12 (Table 1). A similar minor effect was observed for the exchange of Cys in position V:09 (which holds a Cys in only 4%) to Ala (Table 1).

ArgII:20 Is Important for the Constitutive Activity of EBI2. Emerging evidence suggests that residues pointing into the *minor* binding pocket or residues located elsewhere in the helices confining the minor binding pocket (TM-1, -2, -3, and -7) are also important for receptor activation (Rosenkilde et al., 1994; Zhou et al., 1994; Govaerts et al., 2001a; Miura and Karnik, 2002; Govaerts et al., 2003). Position II:20 usually contains an aromatic residue (31%) or a Leu (20%), and only rarely an Arg (7%) or a Lys (4%) (Mirzadegan et al., 2003). Upon introduction of an Ala in II:20, we observed a substantial decrease (11-fold) in the measured CREB-activity (Fig. 6B) and a 1.4-fold decrease in surface expression (Fig. 6C). The relative constitutive activity for this mutation was therefore decreased 7.1-fold relative to wt (Fig. 6A). In contrast, introduction of a charge-conserving Lys had no effect on the activity, whereas introduction of a charge-reversing Glu resulted in a major reduction in activity (3.8-fold) compared with wt EBI2 (Fig. 6A). Three other residues on the same side of TM-2 were also mutated into Ala (LeuII:17 and PheII:13, located one and two helical turns below ArgII:20, respectively, and TyrII:24, located one helical turn above) with no effect on the activity of EBI2 (Table 2). This clearly indicates that charge is important and that ArgII:20 does not act in concert with any other residues in TM-2 for the maintenance of high constitutive activity. In contrast to the mutations in TM-6 (Figs. 3C and 5C, Table 1), there were no major changes in receptor surface expression for the mutations in TM-2 (Fig. 6C, Table 2).

Putative ArgII:20 Electrostatic Partners: Anionic Extracellular Loop-2 Residues. No obvious electrostatic partners for ArgII:20 are present at the same horizontal level in EBI2 (Fig. 1A). However, in extracellular loop-2 (ECL2), which is constrained near the membrane surface through a disulfide-bridge to the conserved CysIII:01, a total of five Glu residues are present (Fig. 1A). Glu^{183} is located closest to Cys^{181} in ECL2 (which forms the disulfide-bridge to CysIII:01), and was therefore substituted to Ala, (E183A)-EBI2. Although this mutation resulted in a 1.3-fold decrease in the relative constitutive activity, this clearly did not even approach the effect of ArgII:20. Furthermore, the four additional anionic amino acids located either before Cys^{181} (Glu^{175} and Glu^{177}) or after (Glu^{188} and Glu^{189}) were substi-

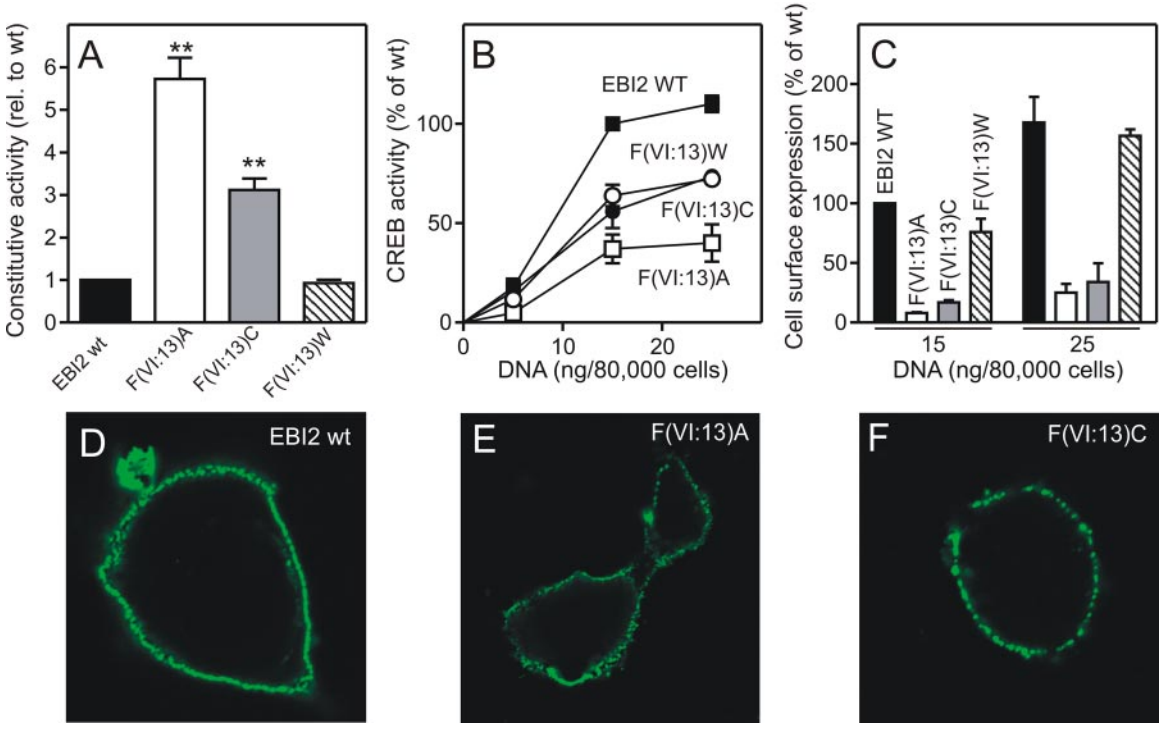

Fig. 3. PheVI:13 in the conserved CFxP-motif is important for the regulation of constitutive activity. HEK293 cells were transiently transfected with Gqi4myr, the reporter plasmid (CREB/Luc system) and increasing concentrations of FLAG-tagged EBI2 receptor (0, 5, 15, and 25 ng/8 $\times$ 10^4 cells). A, the relative constitutive activity of the Ala, Cys, and Trp-introductions in VI:13: F(VI:13A)-, F(VI:13)C-, and F(VI:13)W-EBI2 were calculated from the observed CREB-activation (B), correlated to cell-surface expression (C). The CREB-activation was determined for 0, 5, 15, and 25 ng of receptor/8 $\times$ 10^4 cells (B), whereas the cell surface expression was determined at 15 as well as 25 ng of receptor/8 $\times$ 10^4 cells. The relative constitutive activity was determined for both concentrations (see Table 1), and the values for 15 ng/8 $\times$ 10^4 cells are depicted in A. All experiments (in B and C) were performed in parallel, and wt EBI2 was included in all experiments (N >3). D–F, confocal microscopy of EBI2 wt (D), F(VI:13)A- (E), and F(VI:13)C-EBI2 (F). In brief, HEK293 cells were transiently transfected with 150 ng of receptor /8 $\times$ 10^4 cells, fixed 48 h after transfection, and the cell surface EBI2 expression visualized by the anti-FLAG M1 antibody followed by the Alexa Fluor 488-conjugated IgG antibody. The confocal microscopy was performed using a LSM 510 laser scanning unit coupled to an inverted microscope with an oil immersion Plan-Apochromat objective (Carl Zeiss).

tuted to Ala in a pair-wise manner with no decrease in the constitutive activity of EBI2 (Table 2). In fact, a minor increase was observed for the (E188A;E189A)-EBI2 mutation (1.3-fold compared with wt EBI2). Consequently, the two double mutants were combined with (E183A)-EBI2 creating the two triple-mutants (E175A;E177A;E183)-EBI2 and (E183A;E188A;E189A)-EBI2. The former had the same minor effect as (E183A)-EBI2 (1.4-fold decrease in activity), whereas the latter resulted in a 1.8-fold decrease (Table 2). All in all, these substitutions indicate that the Glu residues in ECL2 do not act in concert as anionic partners with ArgII20 (Table 2 and Fig. 6A).

Putative ArgII:20 Hydrogen Bond Interaction Partners: Residues in TM-3 and -7. Due to the rather inconclusive results in identifying anionic partners, we searched for possible hydrogen bond interacting partners in TM-3 and -7 for ArgII:20. In TM-7, AsnVII:10 (Asn^{298}) has the chemical properties and proper horizontal locality to make hydrogen bonds with ArgII:20 and is in fact infrequently occurring at this position (1%). However, Ala introduction in VII:10 had no effect on the constitutive activity (Table 2). Two additional residues in TM-7 with hydrogen-bonding capabilities, HisVII:03 (His^{293}) and CysVII:14 (Cys^{302}), were mutated to Ala, yet again with no effect on the activity of EBI2 (Table 2). In TM-3, ThrIII:04 is pointing toward TM-7 and TM-2 and is capable of hydrogen bonding. However, no effect was observed upon introduction of Ala (Table 2). In contrast, introduction of Glu in III:04 (in an attempt to force TM-3 closer to ArgII:20 through a salt-bridge formation) resulted in a minor increase in activity (1.4-fold).

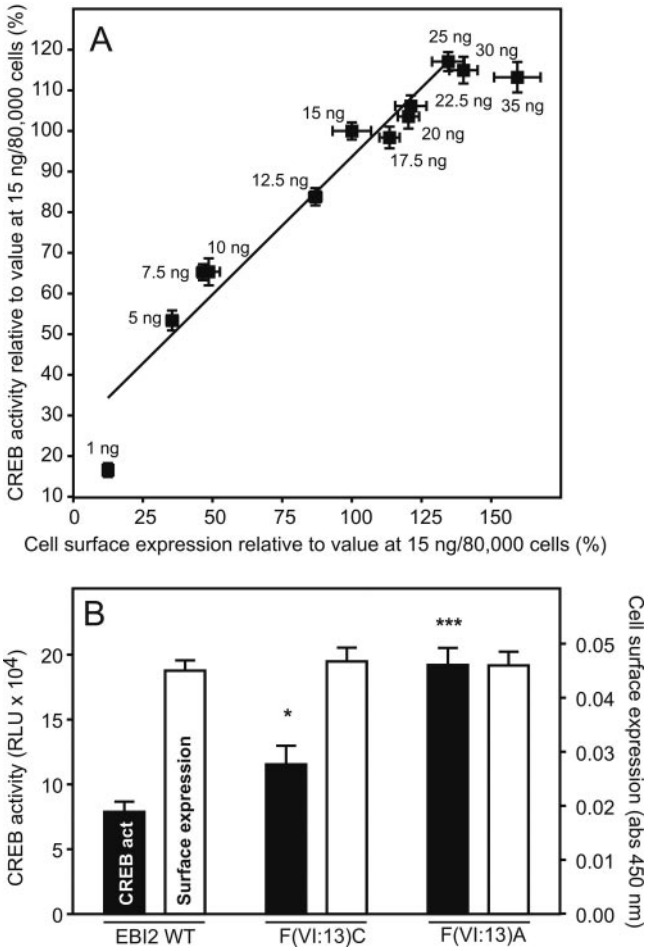

Fig. 4. Correlation of receptor activation and surface expression for multiple DNA concentrations. A, HEK293 cells were transiently transfected with Gqi4myr, the reporter plasmid (CREB/Luc system) and 12 concentrations of FLAG-tagged wt EBI2 receptor (0–35 ng/8 × 10^4 cells), and the activity was determined in parallel with surface expression for all DNA concentrations. A linear regression of the data is indicated by the line. Supplemental Fig. 1 shows the corresponding individual experiments. B, data extracted from similar gene-dose experiments with the Ala and Cys-introduction in VI:13, where the white columns indicate receptor expression, and the black columns indicate receptor activity. Supplemental Fig. 2 shows the correlation for all included DNA concentrations ($n > 3$).

Beneficial Effect of an Electrostatic Interaction between Position II:20 and III:03. Because of the apparent beneficial effect of a Glu at position III:03, a model was built based upon the crystal structure of rhodopsin using SWISS-MODEL (http://swissmodel.expasy.org/SWISS-MODEL.html) and Deep Viewer ver. 3.7 software, and residues in the proximity of ArgII:20 were identified by increasing the search radius from 1 to 5 Å in steps of 0.5 Å. Using this approach, IleIII:03 appeared at a radius of 4 Å, whereas ThrIII:04 appeared at 4.5 Å. Consequently, IleIII:03 was mutated to Ala, Glu (as an attempt to introduce a salt-bridge to ArgII:20), and Arg (to create repulsion to ArgII:20) (Fig. 6, D–F). Whereas the Ala introduction had no effect on EBI2 activity, the Glu introduction resulted in a major *increase* in constitutive activity (4.4-fold relative to wt EBI2) in contrast to a major decrease in case of the Arg in III:03 (4.6-fold) (Fig. 6, D–F). These results together indicate a possible interaction between ArgII:20 and IleIII:03, in that the introduction of Glu in III:03 (+/−) increased the constitutive activity through a putatively formed salt-bridge, whereas the Arg introduction at III:03 (+/+) prevented activity through repulsion [(*x*/*y*) designates the charges at II:20 (*x*) and III:03 (*y*), in which "+" is positive, "−" is negative, and 0 is neutral].

Exchange of Charges in Position II:20 and III:03. To substantiate the beneficial effect of the (+/−) electrostatic interactions (Fig. 6D), we swapped charges (−/+) by combining the two signaling-deficient single-mutations: R(II:20)E-EBI2 (−/0) and I(III:03)R-EBI2 (+/+) (Fig. 6, A and D, respectively). The resulting double mutation (−/+) increased the constitutive activity 2.7-fold relative to wt (Fig. 7A), whereas, as expected, the double-mutant (−/−) created by Glu introductions at both positions decreased the activity (Fig. 7A) [similar to (+/+); Fig. 6D]. In contrast to the almost unaltered surface expression for the mutations of ArgII:20 (Fig. 6C), we observed a huge decrease for the mutations of III:03, especially for the Glu- and Arg-introduction (6.0% and 19% of wt EBI2 expression, respectively) (Fig. 6F). The double mutations obtained by combining these two mutations with the Glu-substitution of II:20 were predictably equally lowly expressed (6.2 and 7.1% of wt EBI2; Fig. 7C). Despite this, however, confocal microscopy uncovered visible and reliable surface expression for all four mutations (Fig. 7, D–G), and adjustment to exactly the same surface expression by varying the DNA concentrations revealed the same phenotype for the mutations in III:03 (Supplemental Fig. 3). Thus, as summarized in Fig. 8, these data strongly suggest that the constitutive activity of EBI2 can be regulated through an interaction between II:20 and III:03, because the single-mutation with Glu introduction in III:03 (+/−) resulted in a 4.5-fold increase in constitutive activity (through electro-

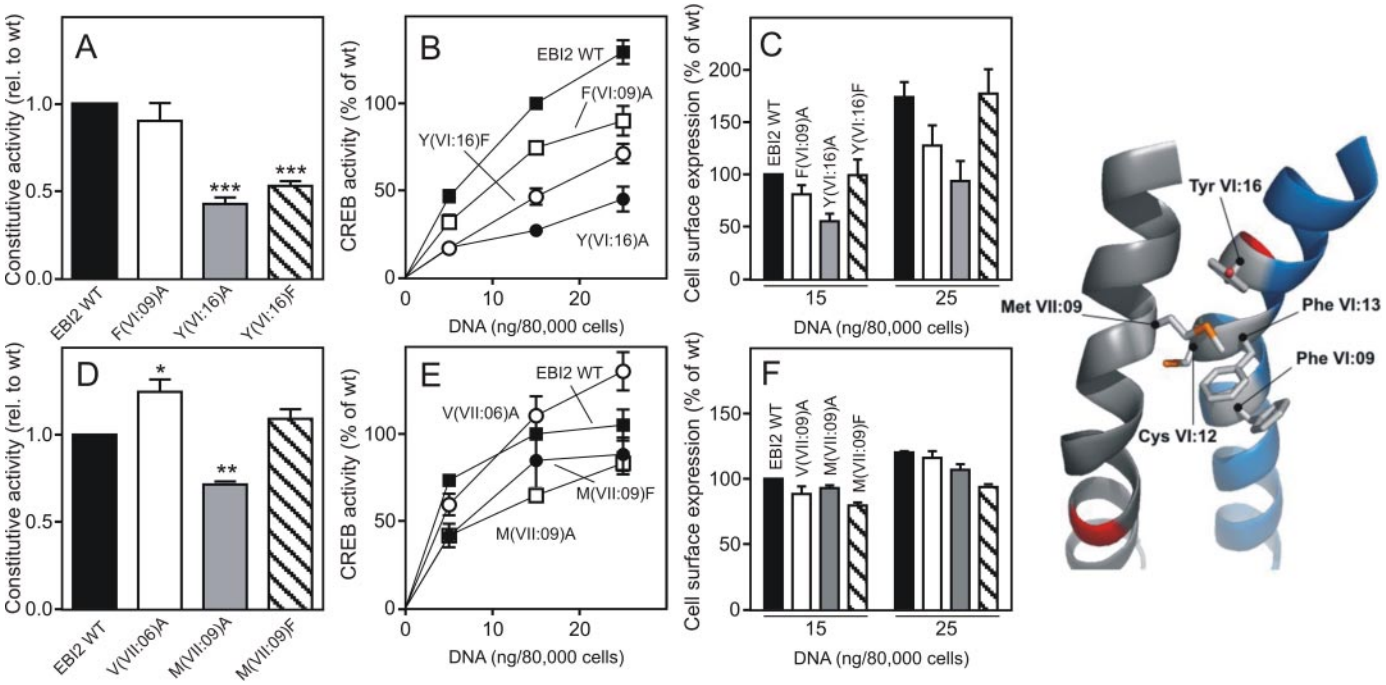

Fig. 5. The role of TM-6 and residues nearby for 7TM receptor activation. The experiments were performed as described in Fig. 3. Relative constitutive activity (A), observed CREB-activation (B), and surface expression (C) for the mutations in the two other aromatic residues in TM-6 (PheVI:09 and TyrVI:16). Relative constitutive activity (D), observed CREB-activation (E), and surface expression (F) for the mutations in TM-7 (ValVI:06 and MetVII:09) ($n > 3$). Molecular model showing PheVI:13 and the surrounding residues in EBI2 based on the crystal structure of rhodopsin and rendered wih PyMOL software. TM-6 (blue) and TM-7 (gray) are seen from the major binding pocket, with the positions of ProVI:15 and ProVII:17 marked in red.

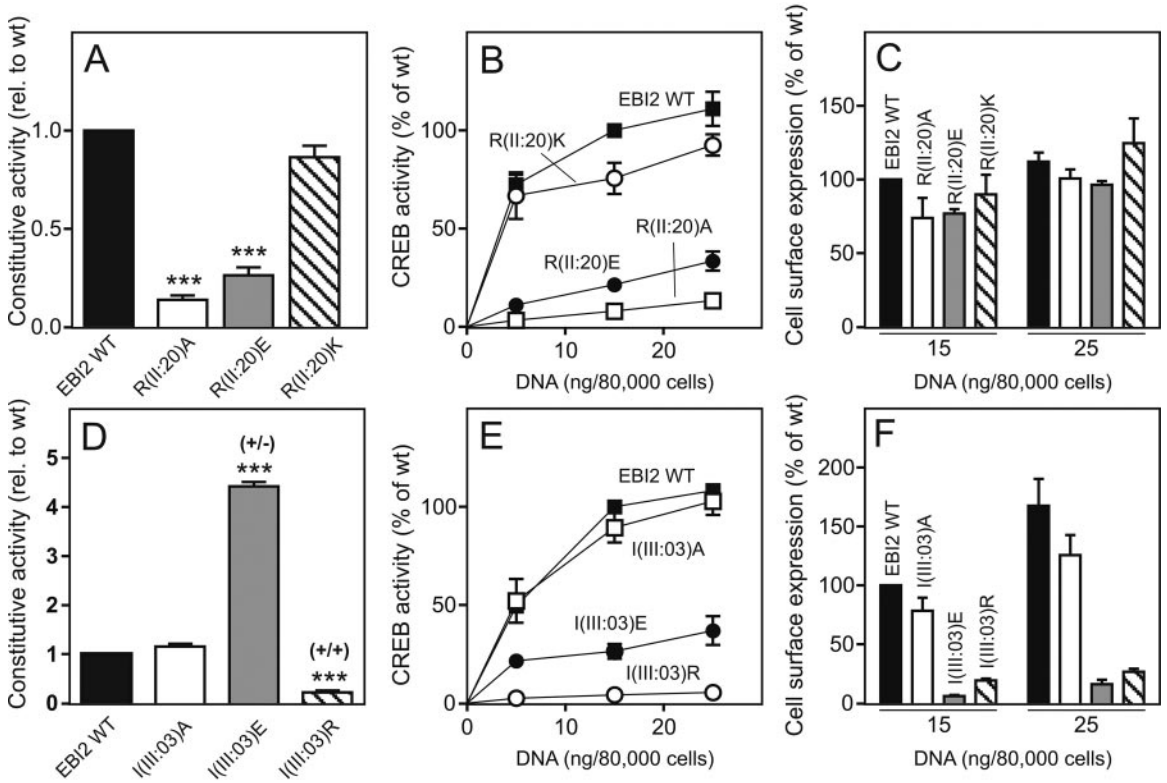

Fig. 6. ArgII:20 is important for EBI2 activity, and interaction with III:03 stabilizes the activity. The experiments were performed as described in the legend to Fig. 3. Relative constitutive activity (A), observed CREB-activation (B), and surface expression (C) for the Ala, Glu, and Lys introduction in II:20 in substitution of Arg. Relative constitutive activity (D), observed CREB-activation (E), and surface expression (F) for the Ala, Glu, and Arg introduction in III:03 in substitution of Ile ($n > 3$).

static interactions with Arg II:20) and that these charges could be swapped (−/+) upon introduction of Glu in II:20 and Arg in III:03 (−/+). It is noteworthy that the latter double-mutation (−/+) rescued the activity (>10-fold) of the corresponding signaling-deficient single-mutations (−/0) and (+/+) that exhibited a 3.8- to 4.5-fold decrease in activity compared with wt EBI2 to a 2.7-fold increase in the relative constitutive activity relative to wt (Fig. 8). Thus, the charge "swapping" (+/−) to (−/+) resulted in an increase in constitutive to almost the same levels as the (+/−). The difference in activity between (+/−) and (−/+) is probably due to the effect of ArgII:20 (Fig. 6).

Effect of ArgII:20 on Gα_i Coupling in the Absence of the Promiscuous G-Protein. An additional approach was used to illustrate the effect of ArgII:20: measurements of receptor-mediated inhibition of forskolin-induced cAMP production. The transcription factor CREB was used as a read-out for the cAMP levels in HEK293 cells (Fig. 9, A–D), and the receptor expression was determined in parallel (Fig. 9, E and F). As seen in Fig. 9A, increasing concentrations of EBI2 DNA (0, 5, 15, and 25 ng/8 × 10^4 cells) inhibited forskolin-induced cAMP-production in a gene-dose-dependent manner, and addition of pertussis toxin totally abolished this effect (as expected from the Gα_i nature of EBI2 signaling) (Fig. 9A). The charge-conserved substitution of ArgII:20 to Lys had no effect on the signaling, whereas introduction of Ala and Glu impaired EBI2 signaling (Fig. 9B). None of the mutations in position II:20 had any huge effect on receptor expression. Introduction of Arg in position III:03 (+/+) impaired EBI2 signaling (charge-repulsion), whereas a Glu at this position (I(III:03)E (+/−) increased the signaling to wt levels (Fig. 9C). Given the very low expression of (I(III:03)E compared with wt (12% of wt; Fig. 9F), the relative activity for this construct was above wt levels (as observed in Fig. 6D). The charge-swapping mutation R(II:20)E;I(III:03)R (−/+) (Fig. 9D) increased the activity of the two signaling-deficient R(II:20)E (−/0) (Fig. 9B) and I(III:03)R (+/+) (Fig. 9C), and given the low expression (6% of wt), the relative activity for this construct was above wt levels (as observed in Fig. 7A). Thus, the effect of ArgII:20, and the beneficial effect of (+/−) and (−/+) obtained by measuring cAMP-levels in HEK293 cells (Fig. 9) were similar to the results obtained using the co-transfection with the promiscuous Gqi4myr (Figs. 6 and 7).

Discussion

The present study focuses on the molecular mechanism behind the constitutive activity of EBI2. Because EBI2 lacks a known ligand, the receptor activity was normalized for surface expression. We analyzed 44 mutations in 29 residues broadly distributed around the major and minor binding pockets and in ECL2 and identified two regions of importance for the constitutive activity. Thus, we found that the middle of TM-6 (CFxP-motif), more specifically PheVI:13, functions as a negative regulator of activity, whereas ArgII:20 functions in the opposite way.

Quantification of Receptor Activity in the Absence of an Agonist. The level of constitutive activity is usually correlated to the maximum agonist-induced stimulation (Holst et al., 2004; Jensen et al., 2007). In the absence of agonists, the receptor activity was correlated to cell surface expression determined by ELISA using antibodies against the M1-FLAG-tag (Figs. 3 and 5–7)—a method also used in other studies (Govaerts et al., 2001b; Srinivasan et al., 2007). Among the multiple receptor DNA concentrations analyzed (Fig. 4A), we chose 15 and 25 ng/8 × 10^4 cells for the corre-

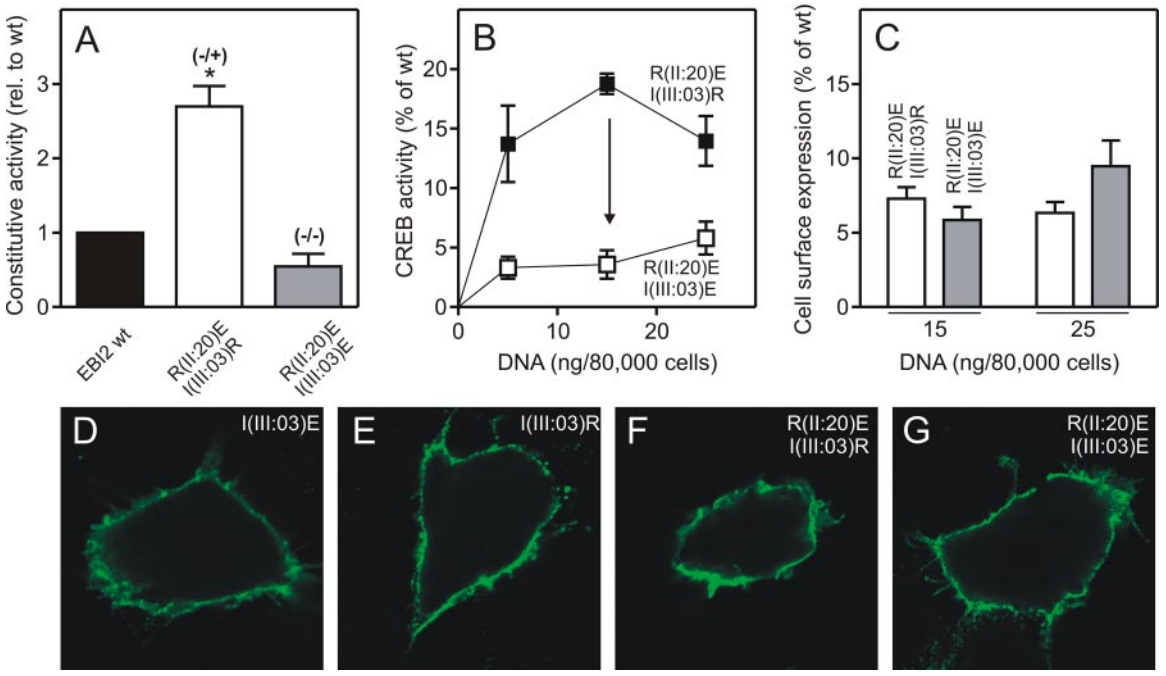

Fig. 7. Charge swap between II:20 and III:03 rescues activity of EBI2. The experiments were performed as described in the legend to Fig. 3. Relative constitutive activity (A), observed CREB-activation (B), and surface expression (C) for the two double mutations: swap of charges [(+/−), shown in Fig. 6D, to (−/+)] by Glu introduction in II:20 and Arg introduction in III:03Ala (white column), and introduction of Glu at both positions (−/−) (gray column) ($n > 3$). Confocal microscopy of the single and double mutations involving Glu and Arg introduction in III:03, either as single mutations (D and E, respectively) or combined with substitution of ArgII:20 to Glu (F and G, respectively). The confocal microscopy was performed as described in Fig. 3.

lations. Certain mutations with major effect on receptor activity displayed very low surface expression [for example, Ala and Cys in VI:13 (Fig. 3C) and Glu and Arg in III:03 (Fig. 6C)]. However, adjusted to the same expression level, we observed similar activity fluctuations as obtained for the fixed (15 and 25 ng/8 $\times$ 10^4 cells) DNA concentrations. Thus, for the two mutations in VI:13, the activity was increased 1.6- to 2.5-fold for equal receptor expression (Fig. 4B, and Supplemental Figure 2) compared with 3- to 6-fold obtained from fixed DNA concentrations (Fig. 3A, Table 1). Likewise, introduction of Glu in III:03 resulted in a 1.5- to 2-fold increase, whereas Arg decreased the activity 5-fold (Supplemental Figure 3), compared with the 4-fold increase and 5-fold decrease obtained for fixed DNA concentrations (Fig. 6D, Table 2).

The Role of TM-6 and Nearby Residues for 7TM Receptor Activation. Movements of TM-6, and to a lesser extent TM-3 and -7, are essential for receptor activation (Farrens et al., 1996; Kim et al., 2004). The CWxP-motif in TM-6 has been identified as a key regulator of movements, the Trp residue acting as a rotameric toggle switch (Schwartz et al., 2006)—putatively in concert with CysVI:12, as suggested for the β2-adrenergic receptor (Shi et al., 2002), or with PheIII:12, as suggested for the cannabinoid CB1 receptor (McAllister et al., 2004). Thus, in many receptors, substitution of the aromatic residue in VI:13 results in abolished activity, for example in the amidergic receptors (Shi et al., 2002), the ghrelin receptor (Holst et al., 2004), and the CaSR (Ca^{2+}-sensing receptor) (Petrel et al., 2003). Position VI:13 in EBI2 contains a Phe that was exchangeable with Trp with no change in constitutive activity (Fig. 3A) and our finding of Phe/TrpVI:13 as a negative regulator (Fig. 3A, Table 1) is in clear contrast to these studies; however, several other 7TM receptors have shown the same phenotype as EBI2. For example, in the bradykinin receptor, a Gln substitution of TrpVI:13 creates constitutive activity (Marie et al., 1999), as does an Ala substitution in CCR8 (Jensen et al., 2007). Furthermore, Trp-to-Ala substitutions result in increased binding or action of agonists or positive allosteric modulators, for example in the CB1 receptor (McAllister et al., 2004), in the CXCR3 receptor (Rosenkilde et al., 2007), and in class C metabotropic glutamate receptor 5 (Muhlemann et al., 2006).

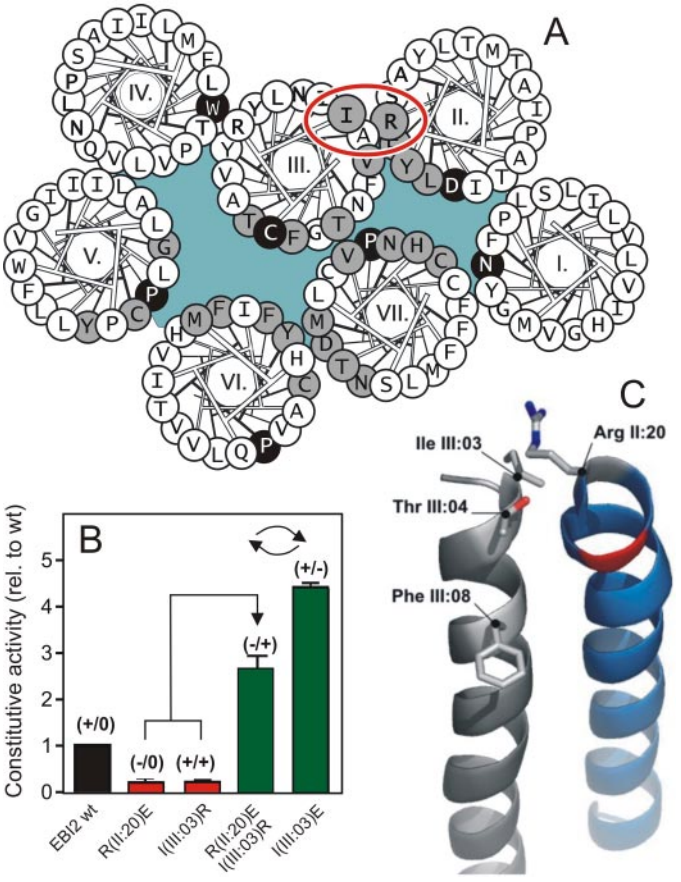

Fig. 8. Summary of the beneficial effect of the electrostatic interaction between position II:20 and III:03. A, helical wheel model emphasizing the positions of interest: II:20 and III:03. B, rescue of the two signaling-deficient single-mutations: Glu introduction in II:20 (−/0) and Arg introduction in III:03 (+/+), embedded from Figs. 6A and 5D, respectively, by combining these two mutations (−/+) (embedded from Fig. 7A) to signaling levels similar to the (+/−) salt-bridge formation from Glu introduction in III:03, embedded from Fig. 3A. C, molecular model showing the proximity of ArgII:20 and IleIII:03 based on the crystal structure of rhodopsin and rendered wih PyMOL software. TM-2 (blue) and TM-3 (gray) as seen from the minor binding pocket, with the positions of ProII:18 marked in red.

Position VI:13 is part of the aromatic cluster including residues in TM-3, -5, -6, and -7 (e.g., III:08 and III:12, V:13, VI:16, VII:06, and VII:09) with importance for signaling in receptors regulated predominantly by small endogenous ligands (Roth et al., 1997; Shi et al., 2002; Holst et al., 2004; McAllister et al., 2004; Schwartz et al., 2006). However, in EBI2, we observed only minor decreases in the activity (1.4- to 2-fold compared with wt) for the Ala substitutions of PheIII:08, TyrV:13, and TyrVI:16, indicating that these aromatic side-chains play only minor roles, at least individually (Table 1). An interesting observation for these three residues was the rank-order of effect being Tyr>Phe>Ala for positions III:08 and VI:16, and Phe>Tyr>Ala for VI:13, indicating that hydrophobicity in addition to polarity matters at these positions. The slight increase in activity for the Met substitution to Phe in VII:09 is consistent with the effect of PheVII:09 (as part of the aromatic cluster) in the ghrelin receptor (Schwartz et al., 2006); interestingly, the increased activity observed for the Ala substitution of CysVI:12 has also been observed in the β2-adrenergic receptor upon introduction of Thr for CysVI:12 (Shi et al., 2002).

ArgII:20—A Major Regulatory Switch for the Activity of EBI2. In general, TM-2 is not considered important for 7TM receptor activation and, in fact, not much attention has been paid to helices confining the minor binding pocket (TM-1,-2,-3, and -7). However, our data suggest otherwise (Figs. 4–9). In particular, the beneficial effect of introducing electrostatic interactions between ArgII:20 (in wt EBI2) and Glu in III:03 (+/−), and the similar beneficial effect of swapping these charges (−/+), whereby the two signaling-deficient single-mutations (−/0) and (+/+) were "rescued" (Fig. 8). In fact, our data do not stand alone. For example, reciprocal mutations between AsnII:16 (Asn^{87}) and AspVII:16 (Asp^{318}) reestablished high-affinity ligand-binding, thereby rescuing the corresponding (deficient) single-mutations in the gonadotropin-releasing hormone receptor (Zhou et al., 1994). Another example is the angiotensin receptor type 1, where it was shown that the orientation of TM-2 changed in constitutively active mutations compared with wt (Miura and Karnik, 2002). Furthermore, the TLP motif (position II:16–18), conserved among most chemokine receptors, has been shown to be important for receptor activation, as mutation of

ThrII:16 to Ala or Val impaired agonist-induced activation in CCR5 (Govaerts et al., 2001a). It is noteworthy that introduction of Lys or Arg, but not Ala in II:16, rendered CCR2 and -5 constitutive active (Arias et al., 2003). Because position II:16 is located one helical turn below II:20, our data correlate very well with these observations. It is possible that the effect of the positive charges in II:16 or II:20 could be ascribed to interactions with negatively charged lipids in the lipid bilayer.

The interaction between ArgII:20 and IleIII:03 in EBI2 is not of a strong nature (no hydrogen bond interaction or salt-bridge formation between Arg and Ile), as supported by the unchanged constitutive activity for I(III:03)A (Fig. 6D and Table 2). It is noteworthy that the importance of TM-II/TM-III interactions has also been observed in other receptors. Thus in CCR5, an interaction of hydrophobic character was shown between PheII:19 and LeuIII:04, because residue swapping rescued a deficient signaling of both single mutations. It is noteworthy that molecular dynamic simulations indicated that II:20 (Trp in CCR5) created stabilizing aromatic interactions with PheII:19, whereas a Leu in III:03 stabilized LeuIII:04 in TM-3 (Govaerts et al., 2003). Thus, viewed from a broader perspective, the upper segment of TM-2 is possibly involved in the stabilization of active receptor conformations, yet no consensus sequence is found in this part of TM-2 or in the surrounding helices (Mirzadegan et al., 2003), which implies that the responsible interaction(s) differ in chemical nature among 7TM receptors. Observations in the NK1 receptor clearly support this notion, because it was shown that Ala substitutions of a series of residues in TM-2 (GluII:10, AsnII:17, AsnII:21, TyrII:24 and AsnII:26) all resulted in an equilibrium-shift between agonist- and antagonist-binding conformations (as measured by B_{max} for radiolabeled agonist and antagonist, respectively)—with ratios of

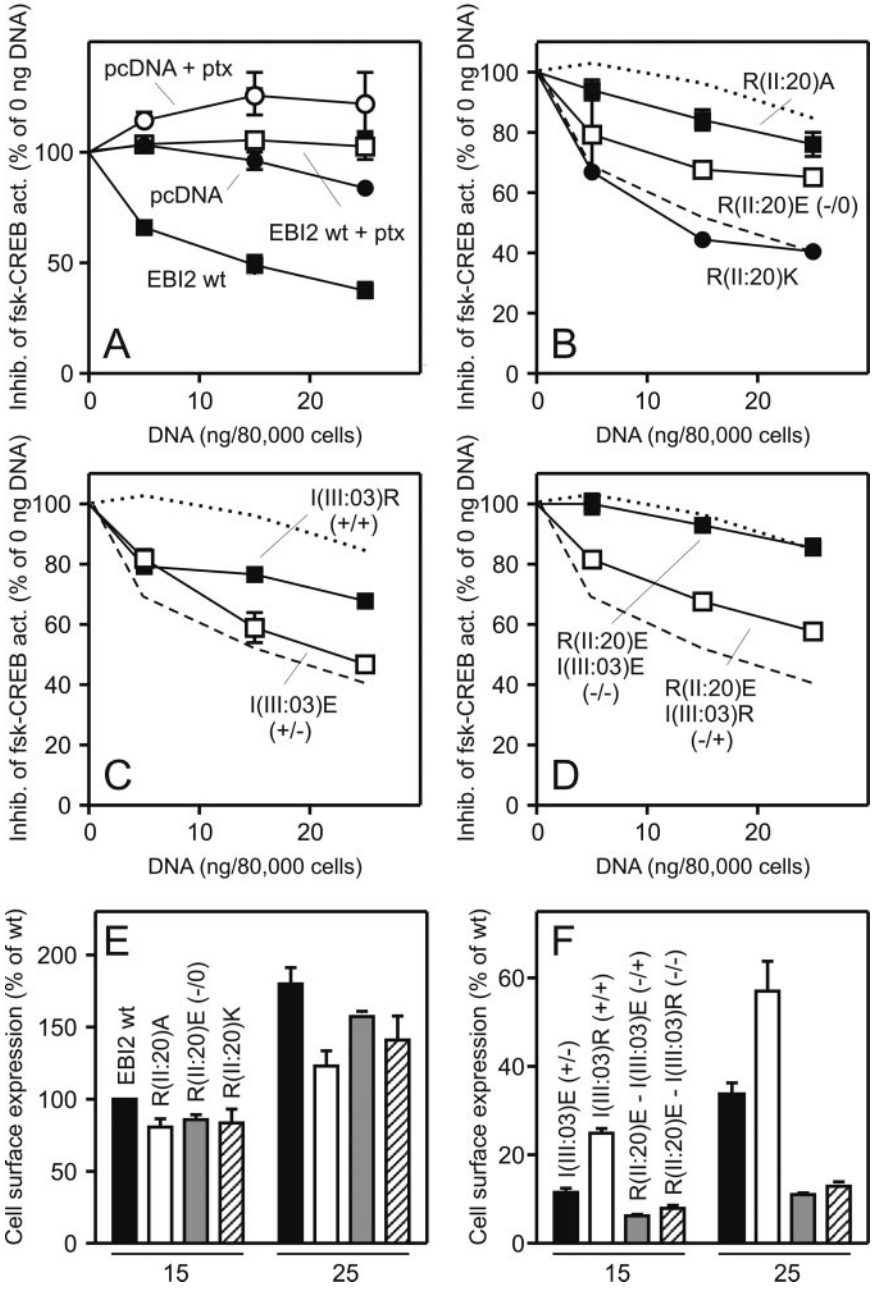

Fig. 9. Inhibition of forskolin-induced cAMP production by EBI2 wt and selected mutants. HEK293 cells were transiently transfected with reporter vector (CREB/Luc system) and increasing concentrations of FLAG-tagged EBI2 wt or mutant contructs (0, 5, 15, and 25 ng/8 × 10^4 cells for A–D and 0, 15, and 25 ng/8 × 10^4 cells for E and F). To stimulate cAMP production, the cells were incubated with forskolin (fsk; 15 μM) and, when present, pertussis toxin (ptx; 100 ng/ml). (Inhibition of forskolin-induced CREB activity by EBI2 wt and pcDNA in the presence or absence of pertussis toxin (A), the II:20 mutants (R(II:20)A/E/K) (B), selected III:03 mutants (I(III:03)E/R) (C), and the double "charge-swap" mutants [R(II:20)E-I(III:03)E (−/−) and R(II:20)E-I(III:03)R (−/+)] (D). The stabled and dotted lines in B–D indicate EBI2 wt and pcDNA (taken from A), respectively. Results are given relative to forskolin-stimulated cells transfected with reporter vector only (0 ng/8 × 10^4 cells) in percentage ± S.E.M. (n = 2–5). E and F, cell surface expression of EBI2 wt and mutants measured by ELISA. Results are given relative to EBI2 wt at 15 ng/8 × 10^4 cells in percentage ± S.E.M. (n = 2–5).

1.1 (B_{max}antagonist/B_{max} agonist) for wt NK1 and 4.0 to 18.5 for the TM-2 mutations (Rosenkilde et al., 1994).

Thus, in summary, the activity of EBI2 is regulated by at least two regions with PheVI:13 and surrounding residues acting as negative regulators, and ArgII:20 acting as a positive regulator.[1] In both regions, it is most likely that the observed effect is due to conformational changes in the receptor and not to a direct interaction with G-proteins in these regions. It is noteworthy that similar effects have been identified in other 7TM receptors for both regions. It is intriguing that the effect of TM-2 is rather similar to that of CCR2 and CCR5, and that the effect of PheVI:13 is similar to that of CCR8 and CXCR3, in that EBI2 has been suggested to belong to the chemokine receptors. However, EBI2 does not contain the Glu in the top of TM-7 (VII:06), or the Glu/Asp and Tyr residues often present in the N termini of chemokine receptors, whereas it does contain part of the conserved TLP in TM-II (ALP in EBI2) and HCC motif in TM-7 (NCC in EBI2). As a final comment, the constitutive active nature of EBI2 implies that it does not "need" any ligand(s) because its activity can be controlled simply by adjusting receptor expression from the promoter region, although the observed increase in constitutive activity suggests that there is still "room" for agonism. Given the cellular expression pattern and the up-regulation by EBV, it is tempting to ascribe EBI2 a future important role as a target for either antiviral or immune therapy. The present uncovering of the molecular mechanisms for EBI2 activation is important from a drug development point of view in that it may facilitate the rational design and development of small-molecule inverse agonists against EBI2.

Acknowledgments

We thank Thue W. Schwartz for fruitful discussions and Laura Storjohann for critical reading. We thank Inger Smith Simonsen and Lisbet Elbak for excellent technical assistance, Ulrik Gether for the use of the confocal microscope, and Peter Baade (7TM Pharma) for assistance with the receptor alignment.

References

Arias DA, Navenot JM, Zhang WB, Broach J, and Peiper SC (2003) Constitutive activation of CCR5 and CCR2 induced by conformational changes in the conserved TXP motif in transmembrane helix 2. *J Biol Chem* **278:**36513–36521.

Bais C, Santomasso B, Coso O, Arvanitakis L, Raaka EG, Gutkind JS, Asch AS, Cesarman E, Gershengorn MC, Mesri EA, et al. (1998) G-protein-coupled receptor of Kaposi's sarcoma-associated herpesvirus is a viral oncogene and angiogenesis activator. *Nature* **391:**86–89.

Baldwin JM (1993) The probable arrangement of the helicee in G protein-coupled receptors. *EMBO J* **12:**1693–1703.

Ballesteros JA and Weinstein H (1995) Integrated methods for the construction of three-dimensional models and computational probing of structure-function relations in G protein-coupled receptors, in *Receptor Molecular Biology* (Sealfon SC ed) pp 366–428, Academic Press, New York.

Beisser PS, Verzijl D, Gruijthuijsen YK, Beuken E, Smit MJ, Leurs R, Bruggeman CA, and Vink C (2005) The Epstein-Barr virus BILF1 gene encodes a G protein-coupled receptor that inhibits phosphorylation of RNA-dependent protein kinase. *J Virol* **79:**441–449.

Birkenbach M, Josefsen K, Yalamanchili R, Lenoir G, and Kieff E (1993) Epstein-Barr virus-induced genes: first lymphocyte-specific G protein-coupled peptide receptors. *J Virol* **67:**2209–2220.

Cherezov V, Rosenbaum DM, Hanson MA, Rasmussen SG, Thian FS, Kobilka TS, Choi HJ, Kuhn P, Weis WI, Kobilka BK, et al. (2007) High-resolution crystal structure of an engineered human beta2-adrenergic G protein-coupled receptor. *Science* **318:**1258–1265.

Elling CE, Frimurer TM, Gerlach LO, Jorgensen R, Holst B, and Schwartz TW (2006) Metal-ion site engineering indicating a global toggle switch model for 7TM receptor activation. *J Biol Chem* **281:**17337–17346.

Farrens DL, Altenbach C, Yang K, Hubbell WL, and Khorana HG (1996) Requirement of rigid-body motion of transmembrane helices for light activation of rhodopsin. *Science* **274:**768–770.

Govaerts C, Blanpain C, Deupi X, Ballet S, Ballesteros JA, Wodak SJ, Vassart G, Pardo L, and Parmentier M (2001a) The TXP motif in the second transmembrane helix of CCR5. A structural determinant of chemokine-induced activation. *J Biol Chem* **276:**13217–13225.

Govaerts C, Bondue A, Springael JY, Olivella M, Deupi X, Le Poul E, Wodak SJ, Parmentier M, Pardo L, and Blanpain C (2003) Activation of CCR5 by chemokines involves an aromatic cluster between transmembrane helices 2 and 3. *J Biol Chem* **278:**1892–1903.

Govaerts C, Lefort A, Costagliola S, Wodak SJ, Ballesteros JA, Van Sande J, Pardo L, and Vassart G (2001b) A conserved Asn in transmembrane helix 7 is an on/off switch in the activation of the thyrotropin receptor. *J Biol Chem* **276:**22991–22999.

Holst B, Holliday ND, Bach A, Elling CE, Cox HM, and Schwartz TW (2004) Common structural basis for constitutive activity of the ghrelin receptor family. *J Biol Chem* **279:**53806–53817.

Hubbell WL, Altenbach C, Hubbell CM, and Khorana HG (2003) Rhodopsin structure, dynamics, and activation: a perspective from crystallography, site-directed spin labeling, sulfhydryl reactivity, and disulfide cross-linking. *Adv Protein Chem* **63:**243–290.

Jensen PC, Nygaard R, Thiele S, Elder A, Zhu G, Kolbeck R, Ghosh S, Schwartz TW, and Rosenkilde MM (2007) Molecular interaction of a potent nonpeptide agonist with the chemokine receptor CCR8. *Mol Pharmacol* **72:**327–340.

Jensen PC, Thiele S, Ulven T, Schwartz TW, and Rosenkilde MM (2008) Positive versus negative modulation of different endogenous chemokines for CC-chemokine receptor 1 by small molecule agonists through allosteric versus orthosteric binding. *J Biol Chem*, in press.

Kim JM, Altenbach C, Kono M, Oprian DD, Hubbell WL, and Khorana HG (2004) Structural origins of constitutive activation in rhodopsin: role of the K296/E113 salt bridge. *Proc Natl Acad Sci U S A* **101:**12508–12513.

Kostenis E (2002) Potentiation of GPCR-signaling via membrane targeting of G protein alpha subunits. *J Recept Signal Transduct Res* **22:**267–281.

Marie J, Koch C, Pruneau D, Paquet JL, Groblewski T, Larguier R, Lombard C, Deslauriers B, Maigret B, and Bonnafous JC (1999) Constitutive activation of the human bradykinin B2 receptor induced by mutations in transmembrane helices III and VI. *Mol Pharmacol* **55:**92–101.

McAllister SD, Hurst DP, Barnett-Norris J, Lynch D, Reggio PH, and Abood ME (2004) Structural mimicry in class a G protein-coupled receptor rotamer toggle switches: the importance of the F3.36(201)/W6.48(357) interaction in cannabinoid CB1 receptor activation. *J Biol Chem* **279:**48024–48037.

Mirzadegan T, Benkö G, Filipek S, and Palczewski K (2003) Sequence analyses of G-protein-coupled receptors: similarities to rhodopsin. *Biochemistry* **42:**2759–2767.

Miura S and Karnik SS (2002) Constitutive activation of angiotensin II type 1 receptor alters the orientation of transmembrane helix-2. *J Biol Chem* **277:**24299–24305.

Mühlemann A, Ward NA, Kratochwil N, Diener C, Fischer C, Stucki A, Jaeschke G, Malherbe P, and Porter RH (2006) Determination of key amino acids implicated in the actions of allosteric modulation by 3,3′-difluorobenzaldazine on rat MGlu5 receptors. *Eur J Pharmacol* **529:**95–104.

Palczewski K, Kumasaka T, Hori T, Behnke CA, Motoshima H, Fox BA, Le Trong I, Teller DC, Okada T, Stenkamp RE, et al. (2000) Crystal structure of rhodopsin: a G protein-coupled receptor. *Science* **289:**739–745.

Parma J, Van Sande J, Swillens S, Tonacchera M, Dumont J, and Vassart G (1995) Somatic mutations causing constitutive activity of the thyrotropin receptor are the major cause of hyperfunctioning thyroid adenomas: identification of additional mutations activating both the cyclic adenosine 3′,5′-monophosphate and inositol phosphate-Ca^{2+} cascades. *Mol Endocrinol* **9:**725–733.

Paulsen SJ, Rosenkilde MM, Eugen-Olsen J, and Kledal TN (2005) Epstein-Barr virus-encoded BILF1 is a constitutively active G protein-coupled receptor. *J Virol* **79:**536–546.

Petrel C, Kessler A, Maslah F, Dauban P, Dodd RH, Rognan D, and Ruat M (2003) Modeling and mutagenesis of the binding site of calhex 231, a novel negative allosteric modulator of the extracellular Ca^{2+}-sensing receptor. *J Biol Chem* **278:**49487–49494.

Rasmussen SG, Choi HJ, Rosenbaum DM, Kobilka TS, Thian FS, Edwards PC, Burghammer M, Ratnala VR, Sanishvili R, Fischetti RF, et al. (2007) Crystal structure of the human beta2 adrenergic G-protein-coupled receptor. *Nature* **450:**383–387.

Robbins LS, Nadeau JH, Johnson KR, Kelly MA, Roselli-Rehfuss L, Baack E, Mountjoy KG, and Cone RD (1993) Pigmentation phenotypes of variant extension locus alleles result from point mutations that alter MSH receptor function. *Cell* **72:**1–20.

Rosenkilde MM, Andersen MB, Nygaard R, Frimurer TM, and Schwartz TW (2007) Activation of the CXCR3 chemokine receptor through anchoring of a small molecule chelator ligand between TM-III, -IV, and -VI. *Mol Pharmacol* **71:**930–941.

Rosenkilde MM, Benned-Jensen T, Andersen H, Holst PJ, Kledal TN, Lüttichau HR, Larsen JK, Christensen JP, and Schwartz TW (2006) Molecular pharmacological phenotyping of EBI2. An orphan seven-transmembrane receptor with constitutive activity. *J Biol Chem* **281:**13199–13208.

Rosenkilde MM, Cahir M, Gether U, Hjorth SA, and Schwartz TW (1994) Mutations along transmembrane segment II of the NK-1 receptor affect substance P competition with non-peptide antagonists but not substance P binding. *J Biol Chem* **269:**28160–28164.

Rosenkilde MM, Kledal TN, Bräuner-Osborne H, and Schwartz TW (1999) Agonists and inverse agonists for the herpesvirus 8-encoded constitutively active seven-transmembrane oncogene product, ORF-74. *J Biol Chem* **274:**956–961.

[1] The modulation of constitutive activity by mutagenesis, and the many different cell- and membrane-based assays for which constitutive activity have been shown (see Rosenkilde et al., 2006) and the GTPγS-binding in Fig. 2 (present work), supports the ligand-independent "constitutive" nature (i.e., that the activity is not caused by an unknown agonist in the medium).

Roth BL, Shoham M, Choudhary MS, and Khan N (1997) Identification of conserved aromatic residues essential for agonist binding and second messenger production at 5-hydroxytryptamine2a receptors. *Mol Pharmacol* **52:**259–266.
Schwartz TW (1994) Locating ligand-binding sites in 7TM receptors by protein engineering. *Curr Opin Biotech* **5:**434–444.
Schwartz TW, Frimurer TM, Holst B, Rosenkilde MM, and Elling CE (2006) Molecular mechanism of 7tm receptor activation—a global toggle switch model. *Annu Rev Pharmacol Toxicol* **46:**481–519.
Seifert R and Wenzel-Seifert K (2002) Constitutive activity of G-protein-coupled receptors: cause of disease and common property of wild-type receptors. *Naunyn Schmiedebergs Arch Pharmacol* **366:**381–416.
Shi L, Liapakis G, Xu R, Guarnieri F, Ballesteros JA, and Javitch JA (2002) β_2 Adrenergic receptor activation. Modulation of the proline kink in transmembrane 6 by a rotamer toggle switch. *J Biol Chem* **277:**40989–40996.
Srinivasan S, Santiago P, Lubrano C, Vaisse C, and Conklin BR (2007) Engineering the melanocortin-4 receptor to control constitutive and ligand-mediated GS, signaling in vivo. *PLoS ONE* **2:**e668.
Vassilatis DK, Hohmann JG, Zeng H, Li F, Ranchalis JE, Mortrud MT, Brown A, Rodriguez SS, Weller JR, Wright AC, et al. (2003) The G protein-coupled receptor repertoires of human and mouse. *Proc Natl Acad Sci U S A* **100:**4903–4908.
Zhou W, Flanagan C, Ballesteros JA, Konvicka K, Davidson JS, Weinstein H, Millar RP, and Sealfon SC (1994) A reciprocal mutation supports helix 2 and helix 7 proximity in the gonadotropin-releasing hormone receptor. *Mol Pharmacol* **45:**165–170.

Address correspondence to: Mette M. Rosenkilde, Laboratory for Molecular Pharmacology, Department of Neuroscience and Pharmacology, The Panum Institute, Copenhagen University, Blegdamsvej 2, 2200 Copenhagen, Denmark. E-mail: rosenkilde@sund.ku.dk